Open Access Library Journal
2024, Volume 11, e11492
ISSN Online: 2333-9721
ISSN Print: 2333-9705

Analyzing Oil Spill Dynamics along the Sudanese Coast Using Web GNOME Modeling

Mahmoud Elmahi[1], Giri Raj Kattel[2,3,4*], Ibrahem M. Abdallah[5], Boufeniza Redouane Larbi[6], Monzer Hamadalnel[7,8], Chabi Nacira[9], El Rhadiouini Charafa[10], Yeboah Emmanuel[10], Ahmed Almahi[11]

[1]School of Atmospheric Sciences, Nanjing University of Information Science and Technology, Nanjing, China
[2]School of Geographical Sciences, Nanjing University of Information Science and Technology, Nanjing, China
[3]Department of Infrastructure Engineering, The University of Melbourne, Melbourne, Australia
[4]Department of Hydraulic Engineering, Tsinghua University, Beijing, China
[5]National Institute of Oceanography and Fisheries, Cairo, Egypt
[6]Institute for Climate and Application Research, Nanjing University of Information Science and Technology, Nanjing, China
[7]Department of Astronomy and Meteorology, Faculty of Science and Technology, Omdurman Islamic University, Oumdurman, Sudan
[8]Joint International Research Laboratory of Climate and Environment Change, Nanjing University of Information Science and Technology, Nanjing, China
[9]Marine and Coastal Ecosystem Laboratory, University Campus of Dely Ibrahim, Algiers, Algeria
[10]School of Remote Sensing and Geomatics Engineering, Nanjing University of Information Science and Technology, Nanjing, China
[11]School of Traffic and Transportation, Beijing Jiaotong University, Beijing, China
Email: gkattel@unimelb.edu.au

How to cite this paper: Elmahi, M., Kattel, G.R., Aballah, I.M., Larbi, B.R., Hamadalnel, M., Nacira, C., Charafa, E.R., Emmanuel, Y. and Almahi, A. (2024) Analyzing Oil Spill Dynamics along the Sudanese Coast Using Web GNOME Modeling. *Open Access Library Journal*, **11**: e11492.
https://doi.org/10.4236/oalib.1111492

Received: March 27, 2024
Accepted: April 27, 2024
Published: April 30, 2024

Abstract

Oil spills pose significant threats to aquatic ecosystems, necessitating the development of accurate predictive models to assess their impact and guide emergency response efforts. This study investigates the potential consequences of oil spills along the Sudanese coast, using the Web GNOME model to simulate two hypothetical scenarios during the winter and summer. The analysis reveals the decisive influence of wind, water currents and temperature on oil spill paths and weathering processes. Winter simulations showed a worrying trend, with spilled oil reaching islands and beaches, while summer scenarios showed minimal risks due to relatively weak and variable wind patterns. We found that the evaporation rates exceeded 60% in both scenarios, while dispersion remained modest. Emulsification processes resulted in a significant increase in the water content in oil molecules within 120 hours of spill initiation. Although this study provides valuable insights into emergency response planning, limitations in the current models still hinder a comprehensive understanding of oil spill dynamics, particularly with respect to wave-induced fragmentation. Further research using diverse spill models is

warranted to improve predictive capabilities and enhance response strategies in the Red Sea region. This study underscores the urgent need to take proactive measures to mitigate potential pollution impacts on Sudanese coastal areas and neighboring islands.

Subject Areas

Petroleum Geology

Keywords

Oil Spill, Web GNOME Model, ADIOS2 Model, Sudanese Coastlines, Red Sea

1. Introduction

Despite the growing momentum towards adopting sustainable energy resources and renewable fuel alternatives to safeguard the degrading environment, the global demand for crude oil continues to persist [1] [2]. Various factors contribute to this sustained demand, notably the recent geopolitical conflicts in Europe and Asia, which have significantly bolstered the need for oil worldwide. Sanctions in trade and blockade of ships have resulted in a huge surge in oil production in some countries, while others are deprived of supplies [3] [4] [5]. For example, the surge in oil production culminated in 3.3 million barrels daily in 2022 alone [6]. However, the escalation in oil production and transportation holds economic benefits and lucrative returns for producing nations, and concurrently heightens the risk of environmental damage in water bodies such as oceans, seas, lakes, and rivers. A surge in both crude oil extraction and transportation has led to incidents of leakage or spillage worldwide, where the vessels traverse to ferry oil from producer to consumer nations [7] [8] [9].

Oil spills refer to the unintentional release of crude oil and its derivatives into water bodies during maritime transportation [10] [11]. Oil spills, which have various reasons of sources, including accidents involving oil tankers, explosions in offshore pipelines, and mishaps during offshore exploration, and refining endeavors, which all pose significant threats to marine and coastal ecosystems [12] [13] [14]. Annually, the marine environments of the world are infiltrated by approximately two million tons of oil, which contains highly toxic and hazardous chemicals [15]. As a result, the oil pollution potentially endangers the marine ecosystem, and can cause adverse impacts, including reversible damages of the biota [16] [17]. Some of the potential impacts being reported globally include the destruction of the vital coral reef systems, marine habitats, and mangroves, largely jeopardizing the ecosystem, biodiversity, and tourism in many affected regions. For instance, the Egyptian Ministry of Petroleum reported that the vessel traversing the Gulf of Suez with persistent purging of engine and dissolution of prehistoric oil reserves along the shorelines have contaminated as long as 160 km in the Egyptian coastline significantly affecting the diverse Red Sea coastal

habitats and the tourist attraction areas [18].

Lately, the rise in industrial activities, including the increased demand for petroleum products and the increased oil tanker movements have brought community awareness in marine and coastal ecosystems conservation and management worldwide. The increased community awareness has further forced many governments to develop appropriate and effective strategies to address the issues of coastal oil spills [19]. A timely and accurate prediction of oil spills, as well as tracked records of their spreads, are crucial to implementing preventivemeasures to reduce their impact on marine and coastal environments [20]. Recently, Mishra & Kumar, (2015) proposed the use of models capable of simulating the path and behavior of oil spills in areas at risk of oil spills. They argue that the mathematical models on oil spills can address the dispersion of oil in seawater by considering it as individual particles, taking into account the external factors such as wind, water current, temperature, and salinity that eventually influence the spread of spilled oil [21].

A mathematical modeling commonly referred to as the Lagrange method has been used for developing better preventive strategies of oil spills worldwide [22] [23] [24] [25] [26]. These models enable timely response to emergencies and facilitate decision-making regarding planning and operations [27]. In addition, they provide important insights into identifying the areas affected by an oil spill. While many scientists have attempted to simulate the oil spill spreads around the world, Sudan still lacks studies of oil spills in its shores and oceans. Hence, this study represents a pioneering effort in analyzing and predicting oil spills in Sudanese waters. It is important to note that most studies of this type have focused on estimating the shortest time for oil to reach the shore based on the model trajectories [28]. For instance, the General Operational Modeling Environment (Web GNOME) developed by the National Oceanic and Atmospheric Administration (NOAA) stands out as the most widely used oil spill model, which is capable of studying the trajectories and fates of oil spills globally, including Sudan in the Red Sea basin [29].

The Red Sea basin has recently witnessed a significant increase in international shipping routes [30]. The Red Sea basin is the main navigation route between the East and the West and has become one of the most important commercial corridors for maritime shipping and transport of crude oil in the Middle East and Africa. Today, about 25% of commercial maritime activities in the world pass through the Red Sea [30] [31]. Given the massive transportation of the oil across the Red Sea basin, Sudanese coasts are becoming more vulnerable to larger oil spills than at any time before. For example, more than 187 million tons of petroleum products crossed the Suez Canal in 2016 alone [32]. Hence, evaluating the repercussions of oil spills in vulnerable areas of the Red Sea area including Sudan has become increasingly necessary to formulate the strategies and plans to be aimed at mitigating the resulting impacts on the coastal environment.

It is worth noting that lately the Sudanese government has also actively parti-

cipated in many international and regional agreements dedicated to protecting the country's marine and coastal environments [31]. Though the establishment of the Seaports corporation 2007, a dedicated marine pollution unit was a positive step in protecting Sudanese waters. The effectiveness of this action pivots timely and accurate oil spill predictions in the region. A precisely trackedoil spill and movement, and the understanding on how they spread, are crucial for implementing the most effective preventive measures and minimizing harm to Sudan's marine and coastal ecosystems, as well as neighboring environments [20]. The Web GNOME model has successfully established the trajectories and fates of oil spills more precisely in the Red Sea and elsewhere [3] [33]. The model's Automated Data Inquiry for Oil Spills Web GNOME tool has a powerful web-based user-friendly interface function so this has been considered the best approach for oil spills prediction in the region [34]. Therefore, by using the Web GNOME model, this study, which is the first of its kind on the Sudanese coast, aims to determine the path and fate of oil spills in the Red Sea basin specifically the Sudanese coast. This initiative is particularly timely given the growing threats of human activities and climate change to the region's delicate marine environment.

2. Materials and Methods

2.1. Study Area

The northeastern region of Sudan, which encompasses the Red Sea State and its capital, Port Sudan, is characterized by a coastal stretch that spans approximately 780 kilometers along the Red Sea (**Figure 1**). This coastal area extends from the Eritrean border at the latitude of 18 degrees south to the Egyptian border at the latitude of 22 degrees north. Port Sudan is an important commercial center, which owes greater significance to its advantageous geographical position along the Sudanese coastline. As per the 2018 census, the population in this particular region was estimated to be around 731,149 individuals [35].

The Red Sea is classified as a tropical enclosed sea located between the continents of Africa and Asia. It connects to the Indian Ocean to the south via the Bab El-Mandeb Strait and to the Mediterranean Sea in the north through the Suez Canal [36]. Today, the Red Sea basin serves as a crucial navigational corridor connecting the East and West, emerging as a pivotal route for maritime shipping and the transportation of crude oil from the oil-rich Arabian region. Due to the substantial volume of oil transported through this region, lately the Red Sea faces a significant risk of potential oil spills [37]. Annually, approximately 15% of the global maritime commerce and 10% of the worldwide seaborne oil pass through the Gulf of Suez via the Suez Canal following the 2015 reconstruction of the new Suez Canal [38]. The coast of Sudan is renowned for its remarkably clear and stunning waters. An extensive network of coral reefs along the Sudanese coast and certain islands such as Dungunab and Sanjaneb features one of the rare natural capitals in the region [39]. Additionally,

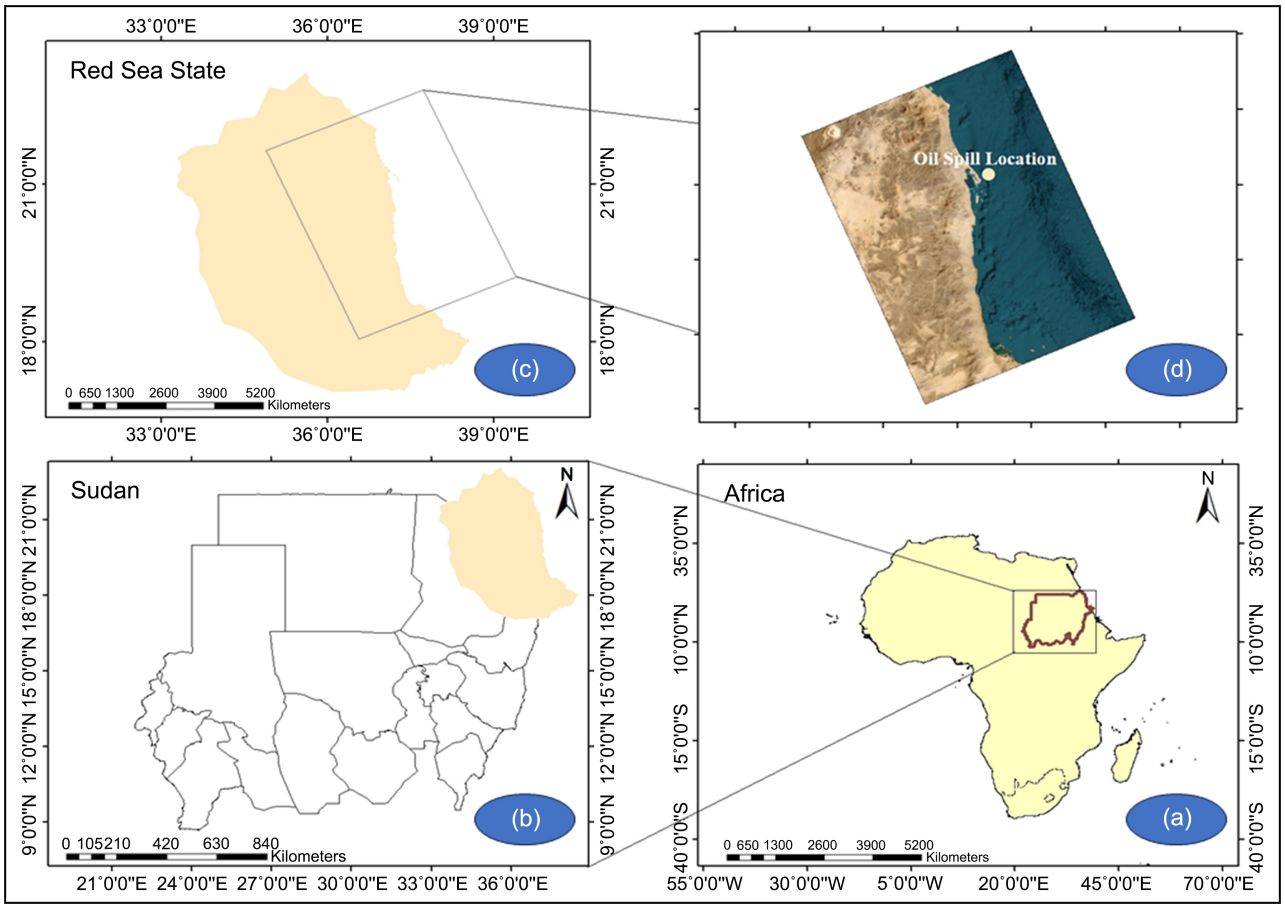

Figure 1. The diagram displays the Sudan's position (b) within Africa (a), highlighting the Sudanese Red Sea State in the northeast (c), acting as Sudan's primary connection to the Red Sea. Additionally, the yellow dot (d) shows the location of the hypothetical oil spill.

there is a widespread presence of mangrove trees in various regions of the Sudanese coastline Dungunab, Sanjaneb and north of the coastline providing significant marine habitats in the region [40]. The two marine reserves, Dungunab and Sanjaneb along the coast, have been officially recognized by the United Nations Educational, Scientific and Cultural Organization (UNESCO) as internationally protected marine parks [41].

However, over the recent decade, a dark cloud hangs over these Sudanese treasures, where the constant threat of oil spills exists in the marine environment from the heavy volume of tankers navigating the Red Sea. As if that weren't enough, Sudan's own bustling import-export scene, particularly involving the oil, adds another layer of risk, with loading activities posing a potential trigger for spills [42].

2.2. Modeling Tools

The frequent instances of pollution and their detrimental effects on the environment from oil spill incidents are what motivate the development of models to predict the movement and fate of oil slicks in continental and marine waters.

These numerical models can simulate numerous scenarios to assess coastal areas of the world including the Red Sea environmental sensitivity before occurrences [43]. Accurate prediction of the direction of the maritime oil spill is essential for coordinating recovery efforts and protecting the polluted areas [44]. The Emergency Response Division (ERD) of the National Oceanic and Atmospheric Administration (NOAA) has been developing oil spill modeling tools for over two decades, including the General NOAA Operational Modeling Environment (GNOME) suite. This updated system consolidates the oil spill fate and weathering tools Automated Data Inquiry for Oil Spills (ADIOS2) and response options into one suite, making it more accessible and powerful, with a new web-based user interface (Web GNOME) [45]. Web GNOME functions as the interface for GNOME and ADOIS2, a publicly accessible model designed to simulate the trajectory and fate of oil spills in coastal and offshore waters [45].

2.2.1. GNOME Model

The GNOME Oil Spill trajectory model is designed specifically for use in both marine and freshwater ecosystems [46]. It is an essential tool for effectively monitoring and reducing the impact of hazardous spill accidents, with a particular emphasis on those involving oil and its byproducts. The model includes important factors such as current, wind, and horizontal mixing, which together affect the movement of an oil slick by controlling the extent of advection and turbulent diffusion [47]. The comprehensive motion of wind and current is ascertained by summing the east-to-west (u) and north-to-south (v) velocity components at each time step (I) through the application of a first-order Runge-Katta technique (forward Euler scheme) [29]. One noteworthy point is that the first-order Runge-Katta method is utilized to calculate the two-dimensional zonal, meridional, and vertical displacements of the influencing factors [34] [48], utilizing the following equations.

$$\Delta x = \frac{\frac{u}{111120.00024}}{\cos(y)} * \Delta t,\ \Delta y = \frac{v}{111120.00024} * \Delta t, \text{ and } \Delta z = 0 \quad (1)$$

In the context of the equations employed u represents the East-West speed ofcurrents and winds, v denotes the North-South speed of currents and winds, y stands for latitude in radians, Δx and Δy represents two-dimensional movements in latitude and longitude, respectively, Δt (where $\Delta t = t - t1$) is the time elapsed between the two steps, discovered that GNOME's inherent limitations prevent it from accurately representing movement between different depth layers, resulting in a constant vertical displacement, Δz, fixed at zero [49]. The equations presented above clarify the function of the GNOME model as an advanced simulation tool specifically created for modeling the dispersion of leaking crude oil or contaminants in Euler currents and wind. The ability to model effectively is attained by integrating Euler-Lagrangian (LES) particles [29] [50]. The model specifically divides the oil slick on the ocean surface and breaks

it down into individual oil particles, each particle is governed by a dynamic coordinate system. Therefore, the motion of these individual oil particles is intimately affected by both the current and the wind conditions that are currently present. It's noteworthy that the GNOME model stands out from other models by requiring a reduced number of input parameters and providing global applicability, as emphasized by Cheng *et al.* [51].

2.2.2. ADIOS2 Oil Spill Weathering Model

Oil weathering is a set of processes affecting spilled oil's chemical and physical properties. The most significant of oil weathering are evaporation, emulsification, and natural dispersion [52]. Oil weathering is a complex interplay of processes, which usually alters the chemical and physical attributes of spilled oil. Hence, the key events driving these transformations include evaporation, emulsification, and natural dispersion [12] [52]. From the moment when the oil diffuses across the water, it is influenced by various hydrometeorological factors including waves, winds, currents, and solar radiation, as well as the specific characteristics of the oil itself such as density, viscosity, and pour point, and the way it is discharged, whether instantaneously or continuously, at the surface or at depth. As a result, a series of processes occur in the water. These processes, which are time-dependent, are directly or indirectly related to the dispersion of the oil and its alteration of properties. Among these time-dependent processes are physical, chemical, and biological mechanisms, including evaporation, dissolution, emulsification and dispersion [53].

As previously stated, the elevated probability of oil spills arises from the escalation in oil exploration and transportation endeavors. Upon discharge of crude oil onto the surface of the sea, a multitude of concurrent processes occur, exerting an influence on its decomposition over a span of time [54]. The ADIOS2 model, designed by NOAA, utilizes real-time environmental data and spilled oil properties to calculate oil weathering processes. It combines a library of 1,000 oils with a short-term oil fate and cleaning model to assess oil persistence in marine environments and recommend cleanup strategies. This model has been employed in various research studies [55]. It elucidates weathering processes through algorithms simulating fundamental weathering processes and their characteristics, including evaporation, emulsification, and distribution. It illustrates the impact of wind speed and water temperature on evaporation rates, the process by which emulsification increases slick size, and how wave energy leads to oil dispersion in the seawater column [55].

2.3. Model Setup and Data Used.

This study simulated potential ship accident scenarios that occur at a hypothetical geographic coordinate: Site (21˚2'40"N, 37˚33'49"E), about 32 km from Dungunab Island. One scenario represents January (winter), and the other scenario represents July (summer) of 2021. The simulations took place over 120 hours. (See **Figure 2**)

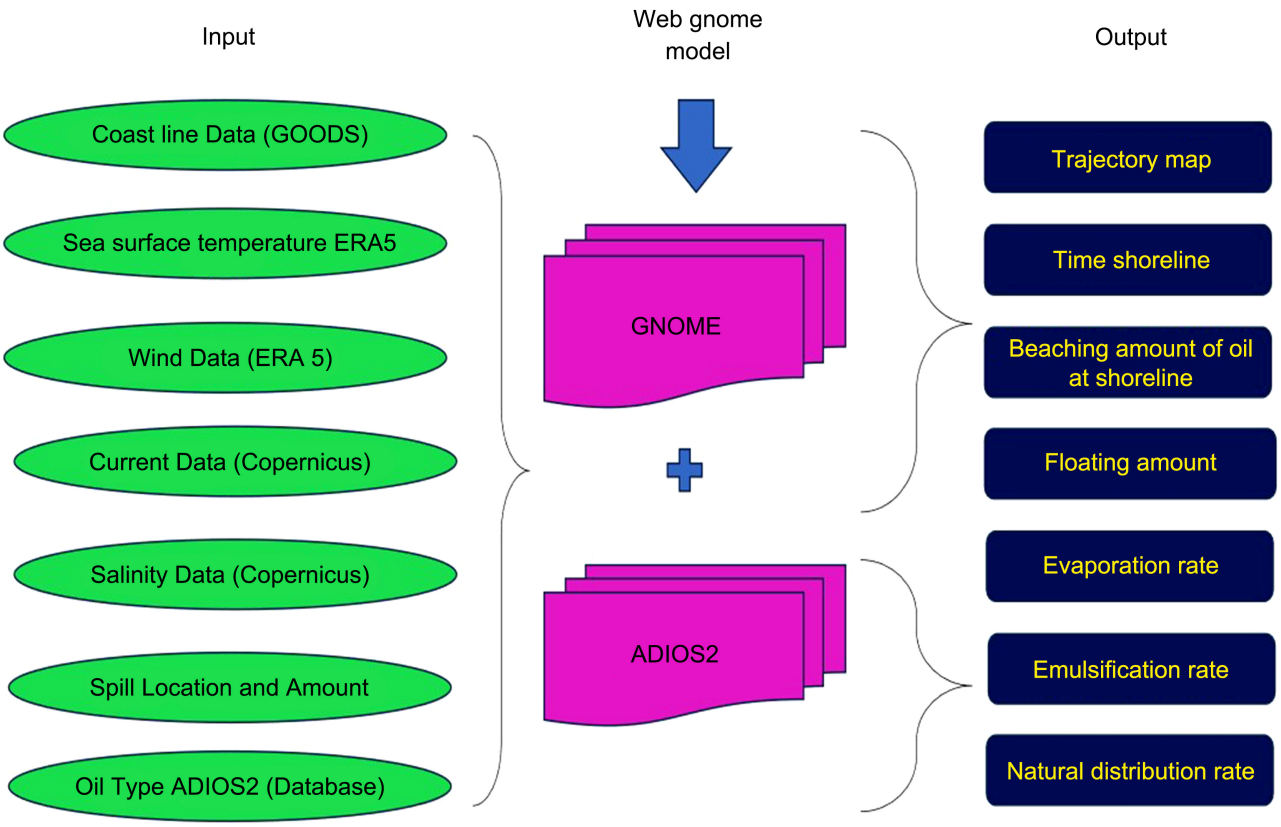

Figure 2. The input and output data diagram framework of Web GNOME (GNOME and ADIOS2) model.

2.3.1. Spill Volume and Oil Type

In this study, we posited the spillage of approximately 1000 metric tons (mt), equivalent to 5000 barrels of Arab Light crude oil, characterized by an API index of 33.4 [28]. This quantity was determined by consultations with experts and adherence to established practices, as delineated in [28]. The selection of Arabian Light crude oil is supported by previous use in studies related to oil spills in the Gulf of Suez-Hurghada [3] [56]. Furthermore, the ADIOS2 Model Library includes a parameter database for this oil type and the characteristic constants necessary to solve the weathering equations.

2.3.2. Coastline Data

The construction of a customized high-resolution vector map delineating the Sudanese coastline was facilitated through the utilization of the Global Self-Consistent Hierarchical High-Resolution Shoreline (GSHHS) database by the National Oceanic and Atmospheric Administration. This map was specifically crafted to define the boundaries of the GNOME model's coastline, which exclusively operates with coastline boundary data in the (BNA) format [44] [57]. The spatial scope of the simulation model encompasses coastal data ranging from 22˚0'0" North to 18˚1'12" South in latitude and from 36˚50'31.2" West to 38˚50'24" East in longitude, thereby covering the eastern-facing segment of the Sudanese coastline along the Red Sea (https://gnome.orr.noaa.gov/#locations).

2.3.3. Sea Surface Temperature

The Red Sea demonstrates substantial variations along its principal axis, often attributed to warmer desert climate [36]. In this investigation, sea temperature data from the monthly ERA5 https://cds.climate.copernicus.eu/cdsapp#!/dataset/reanalysis-era5-single-levels?tab=form dataset was utilized to compute the average temperature over 15 years. Specifically, during January (winter), the average temperature recorded was 26.3˚C, while in July (summer), it escalated to 30.4˚C. The results of calculating the average temperatures agreed with the study by Belkin [58].

2.3.4. Salinity

We calculated the mean salinity over a 15-year period using monthly salinity data obtained from the Copernicus database https://data.marine.copernicus.eu/. The results revealed an average salinity of 38.6‰ in January (winter) and 39‰ in July (summer) 2021. The results of calculating the average temperatures agreed with a study by Megzer *et al.* [59]. The observed elevation in the salinity levels within the Red Sea arises from a confluence of factors. These factors encompass the semi-enclosed nature of the Red Sea, particularly in its southern region where it connects to the Indian Ocean through Bab El-Mandab. Furthermore, elevated water and air temperatures, limited precipitation, increased rates of evaporation, the absence of river inflows, and restricted water exchange with the Indian Ocean collectively contribute to the observed upward trend in salinity [60].

2.3.5. Wind and Marine Currents Data

This study utilized the European Centre for Medium-Range Weather Forecasting (ECMWF) Reanalysis (ERA5) to extract wind data in hourly intervals saved as Network Common Data Form (Net CDF) files. The GNOME model defaulted to a wind factor ranging between 1 and 4%, alongside windage, which accounts for approximately 3% of the surface wind speed, governing the wind-driven movement of the oil [3]. Addressing the data gap in current information, we incorporated data from Copernicus (Global Ocean Physics Analysis and Forecast), as detailed in a preceding study by Abdallah *et al.* [3]. **Figure 3** shows Wind Rose from 2005 to 2022 in port Sudan. The wind was moving mainly in the N, NNE, NW and NNW directions, and the average wind speed reached 10.4 miles per hour.

3. Results

This study simulated the two hypothetical oil spill scenarios from Point Lat 21˚2'40"N, Lon 37˚33'49"E positioned about 32 kilometers to the east of Dunganab Island, utilizing the Web GNOME model, which integrates the GNOME and ADIOS2 models. The subsequent section covers findings concerning oil spill trajectories and the natural oil weathering in the Red Sea area.

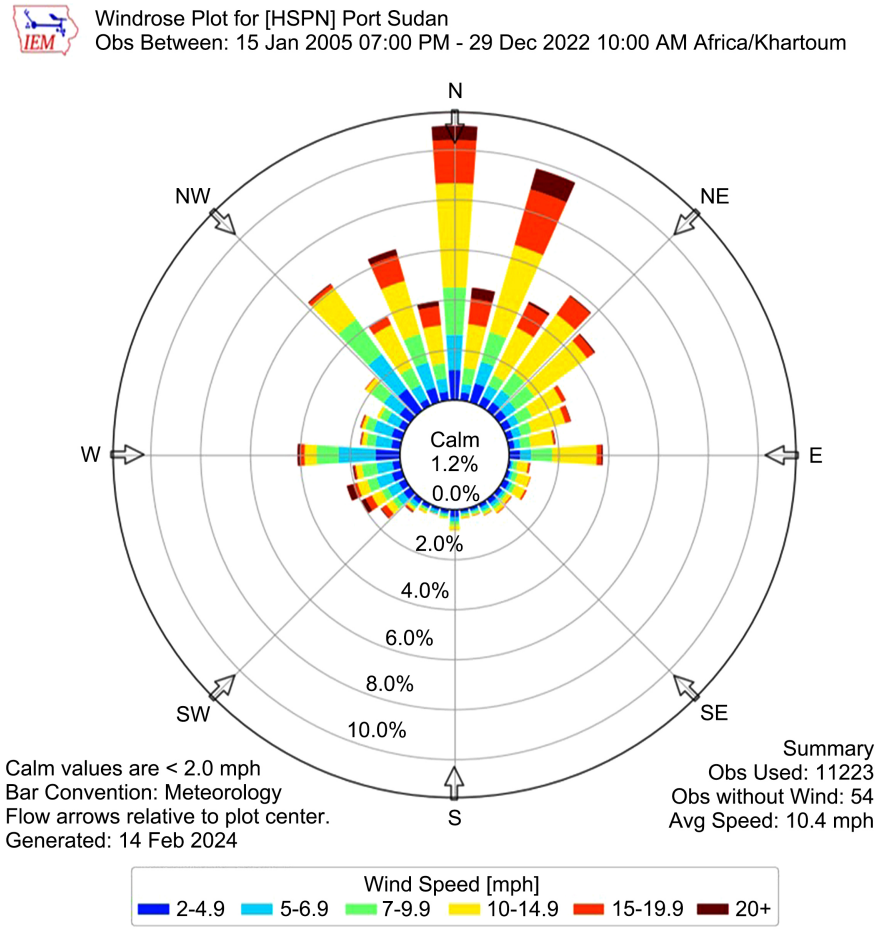

Figure 3. Wind rose diagram at Port Sudan City from 2005 to 2022 [61].

3.1. The First Scenario: January (Winter) 1st, 2021, Trajectory and Weathering

The simulated incident occurred on January 1st, 2021, starting at 00:00:00 and lasting for five days. During this simulation, a quantity of oil was released, approximately 1000 metric tons. The temperature of the sea surface was recorded at 26.5˚C, and the salinity level was measured at 38.6 PSU. This specific site serves as a crucial junction for numerous vessels passing by and is situated approximately 32 kilometers from the (Dunganab) Reserve. Spill movement is illustrated by a set of black and red dots. Black dots indicate the most plausible solution, considering the uncertainty regarding the input parameters. On the other hand, red dots represent the solution with minimal regret, considering uncertainties related to wind and waves. Figures 4-7 exhibit the maps illustrating the simulated progression of the spill every 12 hours. They provide a detailed visual representation of the model's activity in 120-hour intervals.

In Figure 4, the prevailing winds were from the northeast (NE) at an angle of 16.34˚, propelling the spilled oil in the southwest direction at an angle of 196.34˚. These winds continued with varying speeds from 6.3 to 5.78 m/s until 13:45 on January 1st, 2021. At the specified coordinates (Lon 37˚23'14"E, Lat 20˚59'42"N),

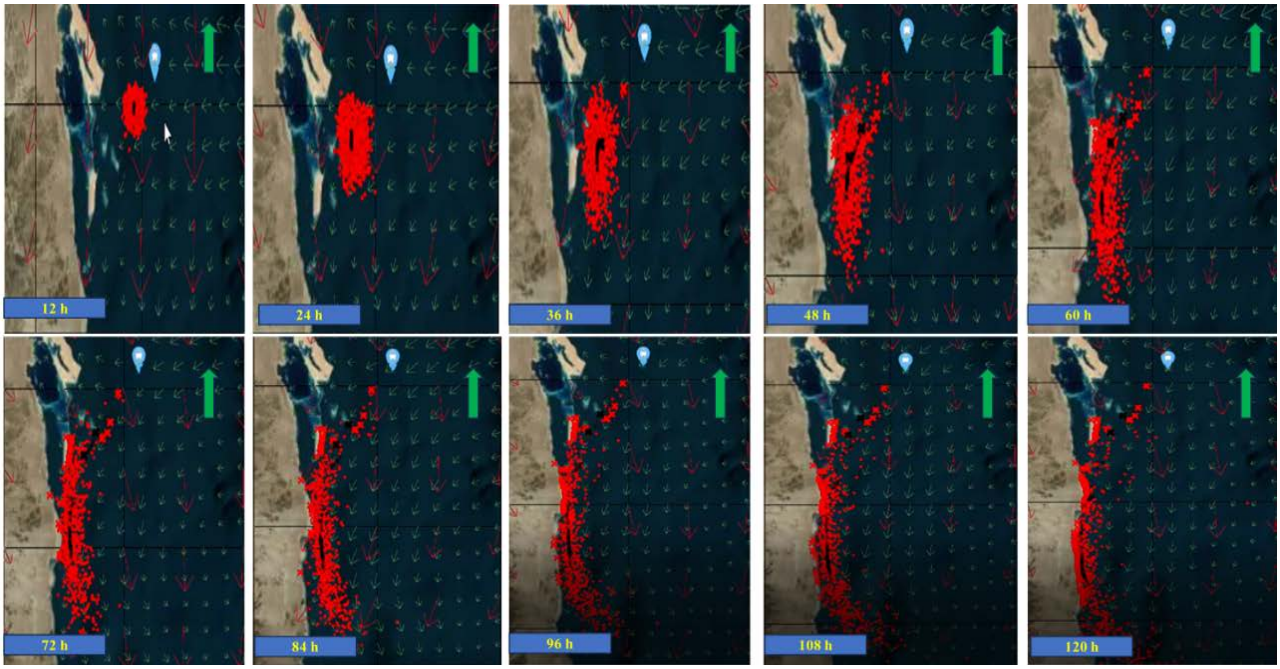

Figure 4. Scenario 1. Modeling the path of movement of oil spill, the small red arrows indicate the wind's direction, while the small green arrows denote the current's direction, with the large blue dot marking the location of the spill.

the oil slick encountered northerly winds from direction (0), prompting the slick to shift southward at an angle of 180˚. The winds then veered to a north-northeasterly direction by 18:00 on January 1st, 2021, continuing into the early hours of the next day at a speed of 5 m/s. By 7:15 on January 2nd, 2021, the initial oil slick reached a small island approximately 24.5 kilometers away from the incident location. The quantity of the initial slick that reached the island totaled 443.3 Kg at coordinates Lon 37˚23'14"E and Lat 20˚51'35"N. Further collisions occurred due to the influence of winds and water currents, resulting in an accumulation of 46 metric tons by 8:30 on January 2nd, 2021. The winds persisted in a north-northeasterly direction at a speed of 5 - 6 m/s, equivalent to 9.72 - 11.66 knots, until 16:00 on January 2nd, 2021. On January 2nd, 2021, at 19:15, the oil slick encountered north winds blowing from a direction of (0), causing the oil to move in the opposite direction (180˚) and leading to another collision with (Magtib) island. These collisions continued until the accumulated oil volume on this island reached 26.21 metric tons (mt) at 14:30 on January 3rd, 2021. The winds persistently directed the oil westwards toward the coast, reaching a quantity of 788.5 kg, equivalent to 0.7885 millimeters per ton, at the point (Lon 37˚14'08"E, Lat 20˚28'19"N) at 11:45 on January 5th, 2021. The north winds continued to propel the spilled oil southward, with a remaining quantity of 314 mt confined between the two points from Lon 37˚13'11"E and Lat 20˚25'30"N and Lon 37˚14'58"E and Lat 20˚8'17"N, estimated at approximately 31 kilometers apart, and approximately 3.5 kilometers away from the coast.

Various weathering processes, including evaporation, natural dispersion, and emulsification, took place at different speeds following oil spills and occur at va-

rying rates in the aftermath of oil spill. Evaporation began quickly after the oil was spilled into the water, and about 4 mt (0.4%) evaporated during the first hour. Over 120 hours, the rate of evaporation steadily rose, ultimately reaching around 600 mt, which accounted for 60% of the total. On the other hand, the process of natural dispersion started one hour after the spill, with an initial dispersion of 2 mt, which increased to 10 mt by the end of the Scenario 1 (Figure 5, Appendix Table 1).

Figure 6 illustrates the emulsion, showing a swift augmentation in water content within the initial hour of oil discharge into the seawater, reaching 85.8% within 24 hours and persistently escalating to 90% by 14:34 on 1/1/2021. The surface volume, including the emulsion, reduced from 1000 mt to less than 652 mt within the first hour and a half. Following that, it experienced a consistent upward trend, ultimately reaching a total of 830 mt on February 2nd, 2021, at 7:15 am. Nevertheless, the percentage subsequently decreased, ultimately reaching a total of 602 mt at the end of the Scenario 1 (Figure 6, Appendix Table 2).

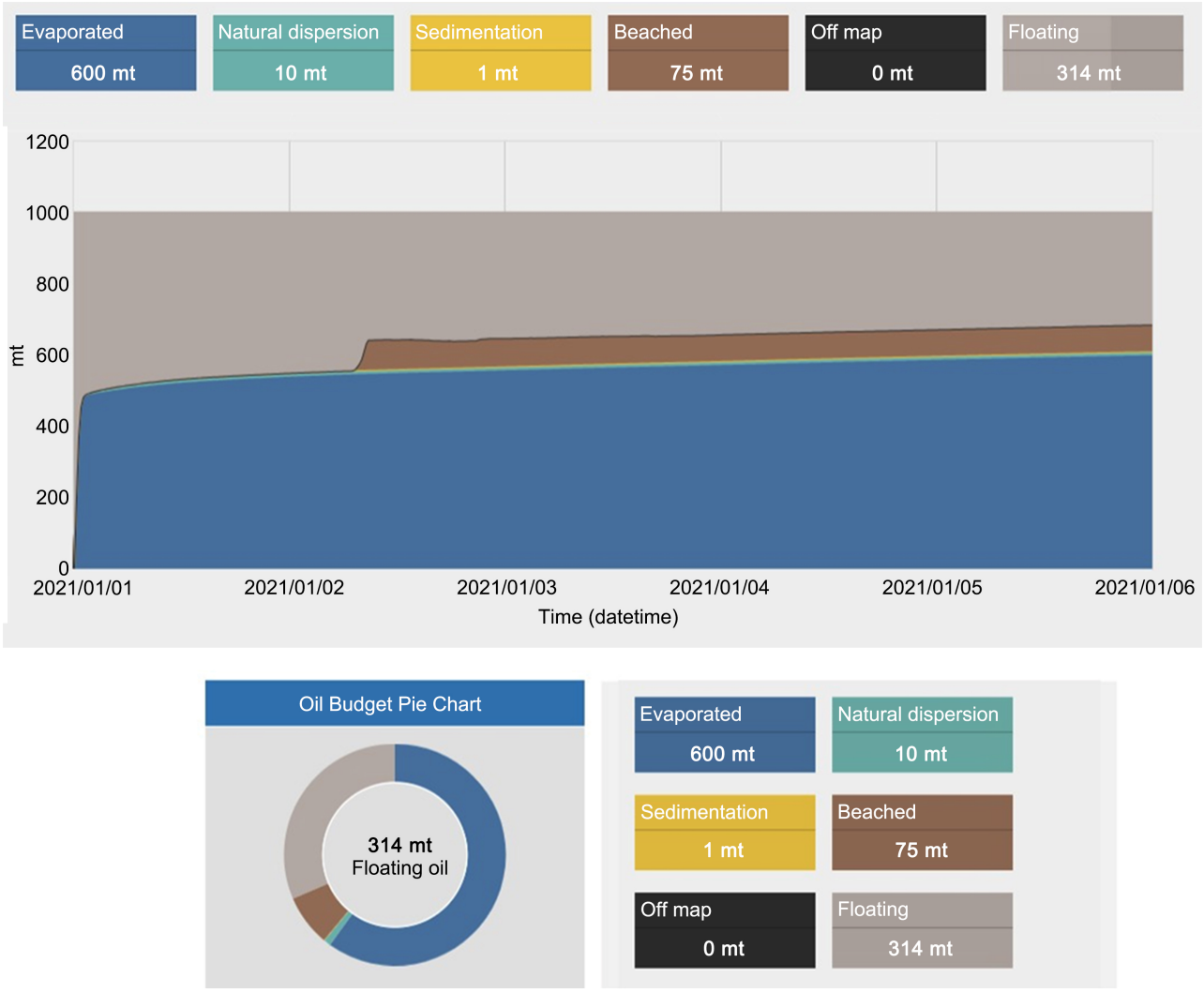

Figure 5. Budget for Arabian Light crude oil in Scenario 1 in January (winter). Unit is on metric ton (mt).

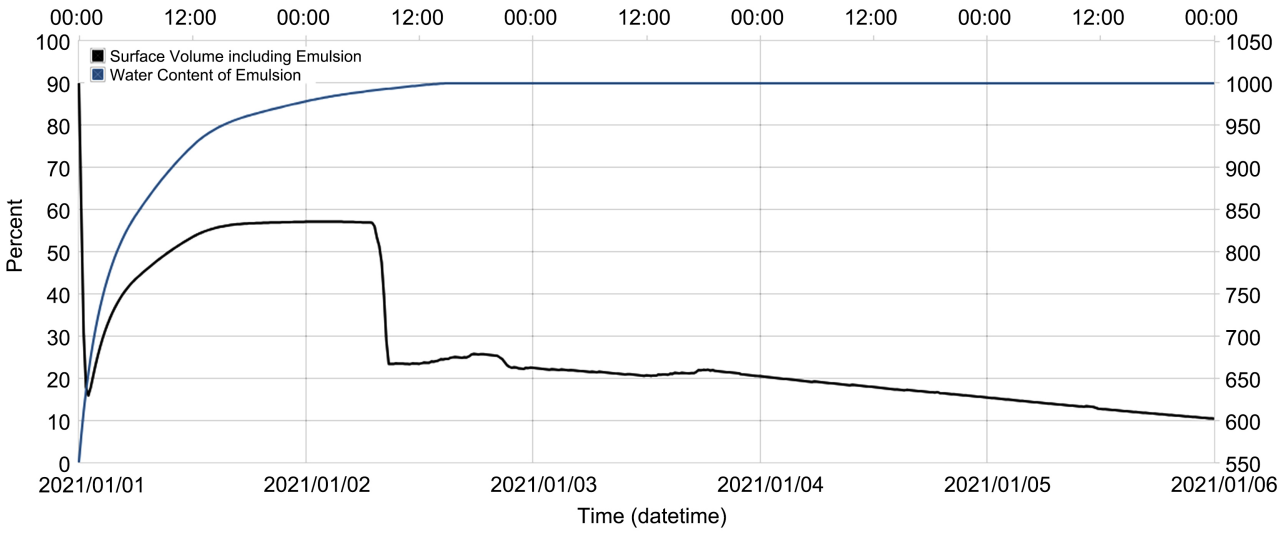

Figure 6. The rate of emulsification for Scenario 1 in January (winter).

3.2. The Second Scenario: July (summer) 1st, 2021, Trajectory and Weathering

In **Figure 7**, the simulation began on July 1, 2021, during the summer season, with a temperature at 30.4˚C and salinity at 39 PSU. The incident began with southwest winds blowing at a velocity of 5 m/s, causing the oil to flow towards the northeast. This movement continued for a period of two hours. Following that, in the coordinates (Lon 37˚38'46"E, Latitude 21˚3'32"N), the oil patch experienced strong winds blowing from the northwest at an angle of 329.80˚, causing the oil to travel to the southeast direction at an angle of 149.8˚ (**Figure 7**). Simultaneously, the water current displayed swift motion at velocities ranging from 27 - 35 cm/sec, moving from a bearing of 272.63˚ to a bearing of 92.63˚, directing the oil along a trajectory towards 152.16˚. The wind consistently blew at a velocity of 5 m/s, causing the oil to follow a trajectory ranging from 140.8˚ to 156.16˚. This pattern persisted until the third day at 14:30 on July 3rd, 2021 (**Figure 7**). By the fourth day, the oil patch started being affected by winds blowing from the northeast and north. These winds caused the oil to move towards the area bounded by the coordinates (Lon 38˚29'1"E, Lat 20˚13'52"N) and (Lon 38˚27'43"E, Lat 20˚8'54"N), without encountering any part of the shoreline. The oil volume contained within this region reached 345 mm/ton at the end of the scenario, spanning an area of 9 km or 5 nautical miles (**Figure 7**).

Immediately after the incident began, evaporation began, leading to the evaporation of 453 mt, equivalent to 45.3% of the total spilled oil, during the first hour. Thereafter, evaporation continued to escalate resulting in a total evaporation of 607 mt of oil, representing 60.7%. By 00:00:00 on the second day, the pace increased continuously, peaking with 646 mt of oil evaporated, representing 64.6% at the end of the scenario. However, dispersion did not occur in the first two hours. After three hours, a small amount (0.1%) of the leaking oil began to spread. The dispersion rate increased steadily, reaching 6 mt at the sixth hour of

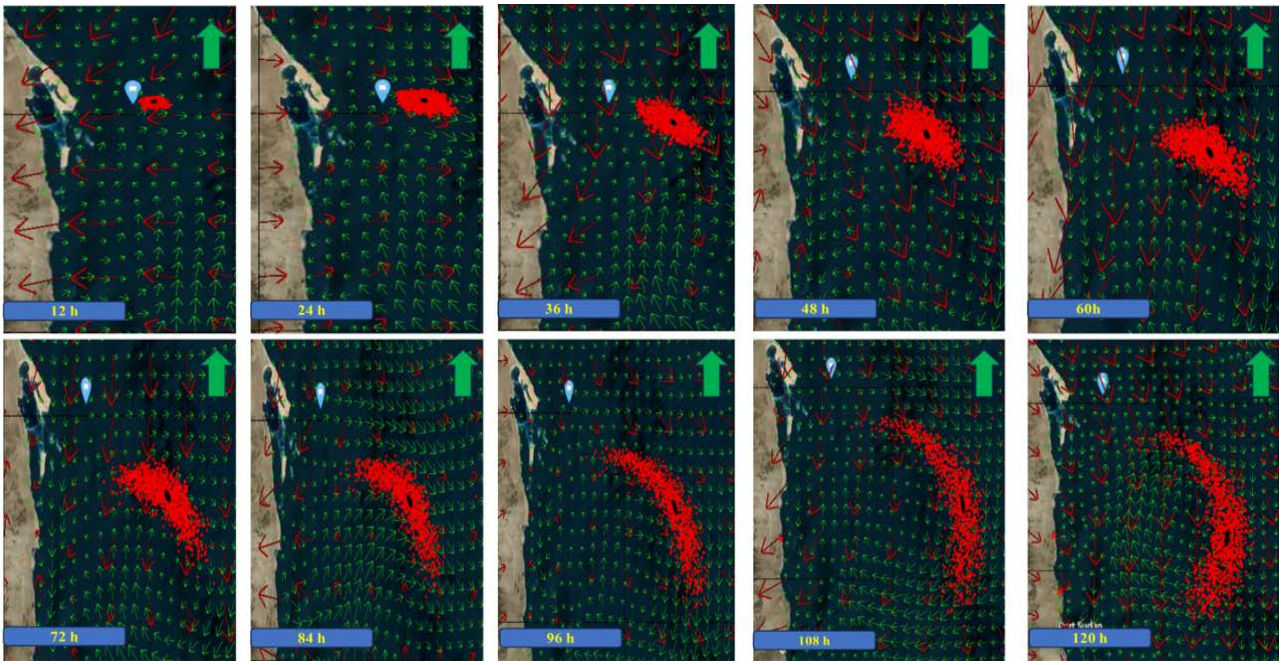

Figure 7. Scenario 2. Modeling the path of movement of oil spill, the red arrows indicate the wind's direction, while the green arrows denote the current's direction, with the large blue dot marking the location of the spill.

the first day. The amount of dispersed oil reached 7.3 mt at 4:14:26 on 07/02/2021, and it continued to increase very slightly until it reached 8 mt at the end of the scenario (**Figure 8**, **Appendix Table 1**).

The surface volume, including the emulsion, first decreased from 1000 mt to 567 mt within the first hour of the spill and continued to decline until it reached 547 mt. At 1:00 on the first day (1/7/2021), the surface volume started to gradually increase, exhibiting a minor upward trend until it reached 640 mt at 7:00. Then, the surface volume exhibited variations marked by both increases and decreases until it peaked at the maximum recorded figure of 682 mt at 23:57:53 on (3/7/2021). After reaching its highest point, the surface volume gradually decreased and ultimately reached a total of 656 mt by the end of the scenario. The water content of the emulsion started to increase at the beginning of the incident and reached 90% after 47 hours and 23 minutes on 7/2/2021. The volume then increased to 1050 mt by the end of the scenario (**Figure 9**, **Appendix Table 2**).

4. Discussion

Oil spills in water bodies can lead to severe impacts on aquatic ecosystems, with potential recovery periods spanning multiple decades, and in some cases, the ecosystem might never fully return to its original state, as indicated by Dhaka *et al.* [62]. Hence, oil spill models are widely used around the world to predict the path and spread of oil, and these results play a vital role in assessing the environmental, economic, and health consequences [63]. Both the oil spill scenarios (Scenario 1 and Scenario 2) simulated on January 1, 2021, and July 1, 2021, provide important insights into the potential consequences and trajectories of oil

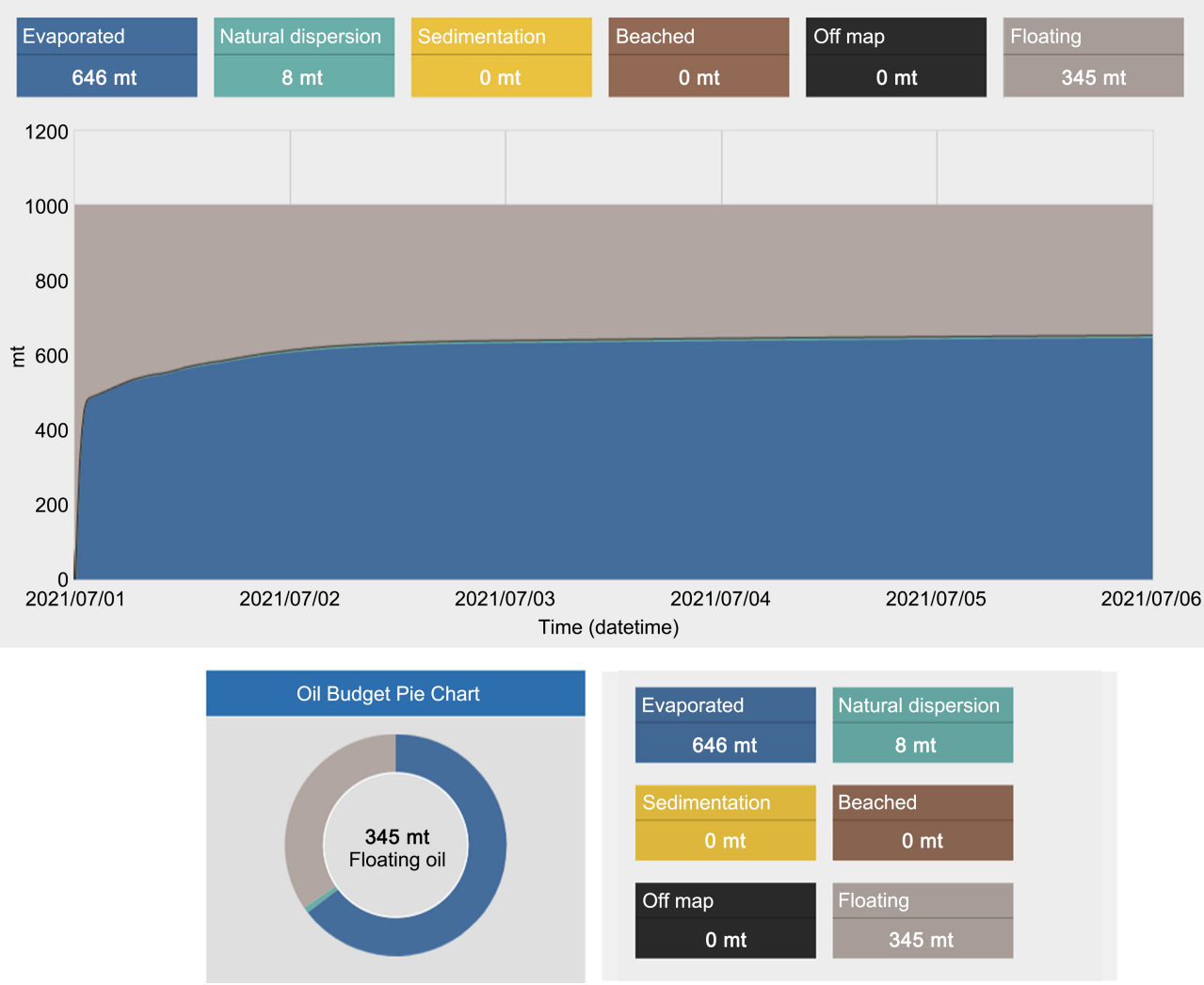

Figure 8. Budget for Arabian Light crude oil in Scenario 2 in July (summer). Unit is on metric ton (mt).

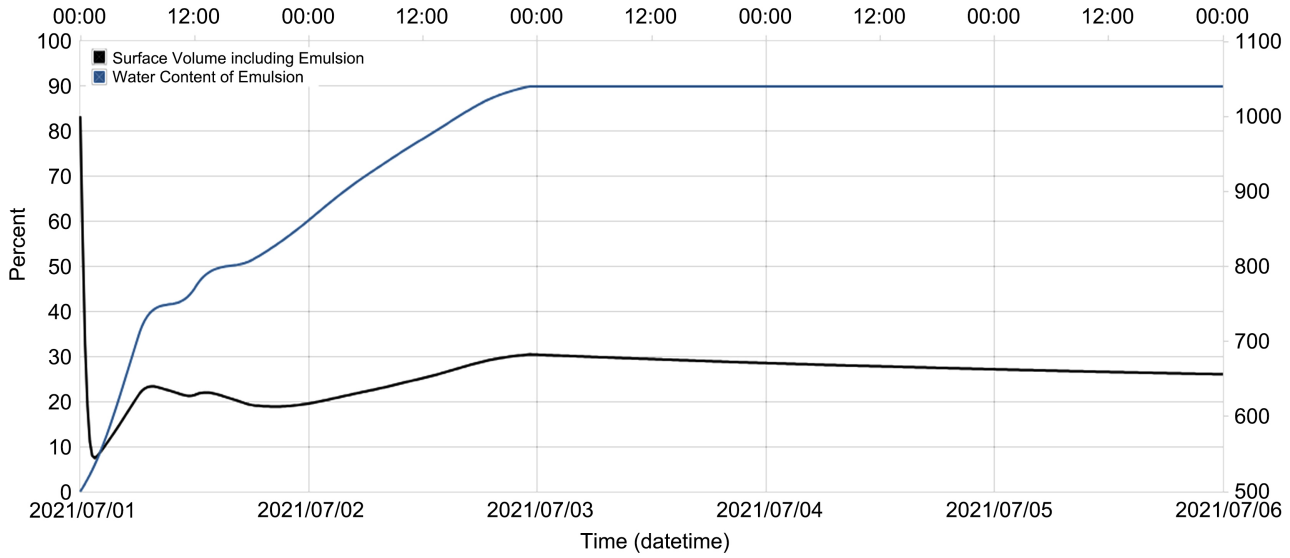

Figure 9. The rate of emulsification for the Scenario 2 in July (summer).

spills in the Sudanese coastlines (**Figure 4**, **Figure 7**). The implications of these scenarios are significant, especially when considering the environmental and ecological impacts in the region. In the Scenario 1, which occurred in January (winter), the spill path was significantly affected by northeasterly winds, causing the oil to bewidespread in a southwest direction. This led to successive collisions with two nearby islands located in the southwest direction from the incident site (**Figure 4**), where the first collision was with an island a little farther away. About 24.5 km from the site of the incident, after 31 hours and a quarter, and the second collision with Muqtib Island occurred 43 hours and a quarter after the beginning of the incident, and then the spilled oil moved southwest towards the coast. A small spot estimated at several kilograms reached the point (Lon 37˚14'08"E, Lat 20˚28'19"N) after which the oil moved furthest, under the influence of the northern winds, to the south at the end of the scenario.

On the other hand, the Scenario 2 in July (summer), showed a different path due to the variable patterns of wind and water currents. We find that the spilled oil was affected at the beginning of the incident by southwesterly winds, which pushed the spilled oil towards the northeast, which is the opposite direction to the islands and the Sudanese coast, and then remained. The oil is under the influence of northwestern winds, northeastern winds, and northern winds, which affected the oil patch to move to the southeast. Which ultimately led to the oil being confined to an area with no connection to the shore. It is about 5 nautical miles from the incident area, and this result is consistent with the result of Abdallah *et al.* [64]. They simulated the oil spill in the Gulf of Suez using the GNOME model and found that when the wind is northeasterly, it pushes the oil in the southwest direction, and also when the wind is northwesterly, it pushes the oil in southeast direction. Our result confirms the decisive role to be played by climates such as winds in directing spilled oil, a phenomenon supported by many studies in the Red Sea and elsewhere [22] [34] [64] [65].

Our results highlight that although the two scenarios occurred at different times (January and July), they confirm the seriousness of the oil spill incidents in the winter on the Sudanese islands and coastal areas, especially since these two islands are located within the borders of the Dunganab Reserve. These islands have tremendous economic and strategic importance, and have been declared as the UNESCO protected areas [66] This study warns that future leaks may harm the entire environmental condition of these islands. As oil spills undergo constant transformation upon contact with water due to weathering. this natural process often generates novel compounds with different physical and chemical properties. However, climate warming in the region may further intensify the condition [58]. Different temperature conditions are found to affect the weathering processes of oil. For instance, at the start, evaporation occurs, and then the more volatile oil components evaporate quickly within a few hours [67] [68]. Higher sea temperatures can accelerate the evaporation of lighter oil fractions, leaving behind heavier, more harmful components that persist longer in the ma-

rine environment. Moreover, warmer temperatures can speed up microbial activity, reducing oxygen levels in the water, adding stress to marine life impacted by the oil spill [69]. Our results showed higher evaporation rates in both scenarios, as evaporation rates in summer were higher than in winter, although higher evaporation rates appeared in the first hours in the winter scenario compared to evaporation rates in the first hours of summer. However, at the end of the scenarios we found that the evaporation rate was much greater in summer than in winter, and this result was consistent with both studies [3] [70]. This may be due to the strength of the winds in the winter compared to the summer, as indicated by Toz *et al.* [71]. We also found that the percentages of remaining oil that got floated at the end of the two scenarios after 120 hours in each of the two scenarios slightly varied, as the amount in winter was 314 mt (31.4%) and in summer was 345 mt (34.5%). The amounts of the remaining oil at the end of the two scenarios during winter and summer are thought to be normal [72]. However, we argue that the difference in evaporation rates in the two scenarios is may be due to the difference in the sea surface temperatures in winter and summer [68]. The difference in the percentage of quantities that remained floating at the end of the simulation can also be explained in both the summer and winter scenarios, as the quantity was greater in summer, while it was expected the percentage in summer would be lower (**Figure 5**, **Figure 8**). This can also be attributed to a reduced summer wind intensity compared to winter. In the winter scenario, 75 mt of oil reached the islands and the coast, whereas in the summer scenario, no oil reached these areas (**Figure 5**, **Figure 8**). This suggests that leaks during winter pose the greatest risk to the Sudanese islands and coasts, given the prevailing winter wind patterns.

The dispersion mechanism inherent to oil spills occurs through the influence of wind and wave energy at the same time, which causes the spills to break up into microscopic, neutrally buoyant droplets and disperse them throughout the air column [73]. In both the winter and summer scenarios, dispersal was nonexistent in the first hour. In the winter scenario, dispersal began an hour after the incident and reached 10 mt by the end of the scenario, representing 1% of the oil spilled (**Figure 5**). Conversely, in the summer scenario, dispersal per hour began at hour 3 of the incident, dispersing 8 mt by the end of the scenario, constituting 0.8% of the total oil spill (**Figure 8**). These percentages are considered modest in both scenarios, and are consistent with the results of Ibrahem *et al.*), who used the (ADIOS2) model and the same amount and type of oil where they recorded a dispersion rate of 1.3% [3]. In our study, we found that the natural dispersion results differ from those of Nasr and Smith, who observed about 8% oil dispersion rate with the SL Ross model [56]. Our model generated a lower dispersion rate, not exceeding 1% in both scenarios (**Figure 5**, **Figure 8**) suggesting that the model difference may be directly related to the difference in wind speeds between the two studies. The wind speed in the Nasser and Smith study area ranged between 10 and 25 knots, while in our region the wind speed

did not exceed 10 knots. This interpretation is supported by the study by Momoh [48]. The study confirmed the possibility of higher dispersion rates on turbulent surfaces, as increasing wind speeds often lead to increased interactions between wind speed, current, and waves, and thus dispersion rates would increase with higher wind speeds [48].

The oil often weathers and loses to its lighter fractions and the remaining heavyweight molecules tend to clump together, forming crystals [74]. These crystals act like tiny anchors, stabilizing the minuscule water droplets within the oil and facilitating the rapidity of emulsions [75]. The water content of emulsions in both scenarios in our study started rising and reached 90% for each indicating both winter and summer climates were sensitive to oil emulsion (**Figure 6**, **Figure 9**). However, the winter scenario reached the emulsifying level faster (38 hours) compared to the summer scenario (47 hours) suggesting that winter in the Red Sea area is more conducive to emulsify the oil particles in the sea. This finding aligns with the study by Hajivand amd Vaziri, which shows that the stable emulsions can contain 60% - 80% water, potentially increasing the spilled material's volume by 2 to 5 times its original size [76]. Oil emulsification has serious effects on surface water as these turn oil spills into a nightmare for cleaning up not only makes the oil thicker and bulkier, but also produces stubborn mousses and tar balls, which greatly increases the challenges of removing oil from the water [62] [77]. The emulsified water is no use for biological refuge either as fish and other biota cannot swim or feed [78]. The understanding of the post-spill behavior of the oil is still far limited inthe study area, but this has become increasingly crucial for a range of responders including humans and fish to oil spills. This knowledge is vital for selecting the most effective tools and tactics to mitigate environmental damage and facilitate cleanup efforts [79].

5. Conclusions

This study examined the critical role of oil spill modeling in understanding the potential repercussions of such incidents in the Red Sea region off the coast of Sudan. By simulating different scenarios across different seasons (winter and summer) it has elucidated the profound influence of wind patterns and water currents on the trajectory and fates of oil spills. Both scenarios have showcased the very oil-reaching vulnerable areas in the region, yet the winter scenario has been found to heighten the environmental risks for the Sudanese islands and coastlines due to the prevailing northeasterly winds. Essentially, the model has divulged several key insights including the pivotal role of wind direction, the heightened evaporation rates during summer and winter due to increased temperature in the area. The low dispersal rates in winter and summer and the exacerbation of emulsification with weathering during winter and summer are also significant. These findings underscore the increased necessity of integrating seasonal weather dynamics into the oil spill preparedness and response strategies in Sudan and the Red Sea in general. Hence, our study further underscores the im-

portance of incorporating climatic changes, such as seasonal variations into the societal actions such as oil spill preparedness and response plans to oil spills in the region. We encourage to explore additional environmental factors and mitigation strategies for optimal protection of sensitive ecosystems in Red Sea area through long-term research on integrated seasonal dynamics of weather patterns and societal response in the future.

For Sudan, highly accurate, modeling tools are needed for real-time data such as wind speed, water currents, and temperature at the time of oil spill incidents along the coast. Deployment of high-frequency radars and buoys canhelp collecting continuous data and model development. To manage oil spill transport along the Sudanese coast, the Government of Sudan, in cooperation with the Sudan Meteorological Authority and the Sudan Sea Ports Authority, which primarily manages oil spills, should immediately address the shortage of marine meteorological stations. Regular and intensive training of staff is urgently needed to ensure rapid response to oil spill incidents. Adequate equipment should be readily available to prevent response delays and protect responders from exposure to hazardous materials. Working with a range of scientists in producing coastal sensitivity mapsofrich environmental and biological diversity along the Sudanese coast is important to avoid further damages.

Acknowledgements

Mahmoud Elmahi would like to express a gratitude to the Sea Ports Corporation Authority of Sudan for providing the opportunity to study leave for China. ME would like to express an appreciation to the Chinese Ministry of Commerce for awarding the M.Sc. scholarship. The Planning and Research Department, the Coastal Station Administration, and the Civil Engineering Department at the Sea ports Corporation Sudan are all highly thankful for sharing the data for this study. GRK would like to acknowledge the Longshan Professorship at NUIST.

Author Contributions

ME, GRK discussed the research idea and study design; ME performed numerical simulations and methodology; ME, GRK, IA, BRL carried out formal analysis, writing and original draft preparation; MH, CN, EC, YE, AA contributed for discussions. All authors have read and agreed for publication.

Conflicts of Interest

The authors declare no conflicts of interest.

References

[1] ITOPF, O.T.S.S. International Tanker Owners Pollution Federation Limited (2011).

[2] Keramea, P., Spanoudaki, K., Zodiatis, G., Gikas, G. and Sylaios, G. (2021) Oil Spill Modeling: A Critical Review on Current Trends, Perspectives, and Challenges. *Journal of Marine Science and Engineering*, **9**, Article No. 181.

https://doi.org/10.3390/jmse9020181

[3] Abdallah, I.M. and Chantsev, V.Y. (2022) Modeling Marine Oil Spill Trajectory and Fate off Hurghada, Red Sea Coast, Egypt. *Egyptian Journal of Aquatic Biology and Fisheries*, **26**, 41-61. https://doi.org/10.21608/ejabf.2022.269676

[4] Adekoya, O.B., Akinseye, A.B., Antonakakis, N., Chatziantoniou, I., Gabauer, D. and Oliyide, J. (2022) Crude Oil and Islamic Sectoral Stocks: Asymmetric TVP-VAR Connectedness and Investment Strategies. *Resources Policy*, **78**, Article ID: 102877. https://doi.org/10.1016/j.resourpol.2022.102877

[5] Adekoya, O.B., Asl, M.G., Oliyide, J.A. and Izadi, P. (2023) Multifractality and Cross-Correlation between the Crude Oil and the European and Non-European Stock Markets during the Russia-Ukraine War. *Resources Policy*, **80**, Article ID: 103134. https://doi.org/10.1016/j.resourpol.2022.103134

[6] Perkins, R. (2022) Global Oil Demand to Surpass Pre-Pandemic Levels in 2022 as Omicron Fears Subside: IEA. S&P Glob. Commod. Insights.

[7] Abereton, P., Ordinioha, B., Mensah-Attipoe, J. and Toyinbo, O. (2023) Crude Oil Spills and Respiratory Health of Clean-Up Workers: A Systematic Review of Literature. *Atmosphere* (*Basel*), **14**, Article No. 494. https://doi.org/10.3390/atmos14030494

[8] Chen, Q., Bao, B., Li, Y., Liu, M., Zhu, B., Mu, J. and Chen, Z. (2020) Effects of Marine Oil Pollution on Microbial Diversity in Coastal Waters and Stimulating Indigenous Microorganism Bioremediation with Nutrients. *Regional Studies in Marine Science*, **39**, Article ID: 101395. https://doi.org/10.1016/j.rsma.2020.101395

[9] Zabbey, N. and Olsson, G. (2017) Conflicts-Oil Exploration and Water. *Global Challenges*, **1**, Article ID: 1600015. https://doi.org/10.1002/gch2.201600015

[10] Kakalis, N.M.P. and Ventikos, Y. (2008) Robotic Swarm Concept for Efficient Oil Spill Confrontation. *Journal of Hazardous Materials*, **154**, 880-887. https://doi.org/10.1016/j.jhazmat.2007.10.112

[11] Mohammadiun, S., Hu, G., Gharahbagh, A.A., Li, J., Hewage, K. and Sadiq, R. (2021) Intelligent Computational Techniques in Marine Oil Spill Management: A Critical Review. *Journal of Hazardous Materials*, **419**, Article ID: 126425. https://doi.org/10.1016/j.jhazmat.2021.126425

[12] Michel, J. (2015) Chapter 7. Oil Spills: Causes, Consequences, Prevention, and Countermeasures. In: Crawley, G.M., Ed., *World Scientific Series in Current Energy Issues*, World Scientific Publishing, Singapore, 159-201. https://doi.org/10.1142/9789814699983_0007

[13] Singha, S. (2014) Offshore Oil Spill Detection Using Synthetic Aperture Radar.

[14] Kachel, M.J. (2008) Threats to the Marine Environment: Pollution and Physical Damage. In: Kachel, M.J., Ed., *Particularly Sensitive Sea Areas*, Springer, Berlin, 23-36. https://doi.org/10.1007/978-3-540-78779-2_2

[15] Ivshina, I.B., Kuyukina, M.S., Krivoruchko, A.V., Elkin, A.A., Makarov, S.O., Cunningham, C.J., Peshkur, T.A., Atlas, R.M. and Philp, J.C. (2015) Oil Spill Problems and Sustainable Response Strategies through New Technologies. *Environmental Science*: *Processes & Impacts*, **17**, 1201-1219. https://doi.org/10.1039/C5EM00070J

[16] Escobar, H. (2019) Mystery Oil Spill Threatens Marine Sanctuary in Brazil. *Science* (80-.), **366**, 672. https://doi.org/10.1126/science.366.6466.672

[17] Magris, R.A. and Giarrizzo, T. (2020) Mysterious Oil Spill in the Atlantic Ocean Threatens Marine Biodiversity and Local People in Brazil. *Marine Pollution Bulletin*, **153**, Article ID: 110961. https://doi.org/10.1016/j.marpolbul.2020.110961

[18] Al-Ghazawy, O. (2010) Red Sea Suffers Crude-Oil Slick. https://doi.org/10.1038/nmiddleeast.2010.175

[19] Dietrich, J.C., Trahan, C.J., Howard, M.T., Fleming, J.G., Weaver, R.J., Tanaka, S., Yu, L., Luettich Jr., R.A., Dawson, C.N. and Westerink, J.J. (2012) Surface Trajectories of Oil Transport along the Northern Coastline of the Gulf of Mexico. *Continental Shelf Research*, **41**, 17-47. https://doi.org/10.1016/j.csr.2012.03.015

[20] Mehanna, A.K., Omar, M.Y., Hassan, A.A., Turki, E.A., Hegazy, E.H. and Elkilani, H. (2013) Modelling of Oil Spill Impacts on Shoreline in Egypt. In: Soares, G. and Peña, L., Eds., *Developments in Maritime Transportation and Exploitation of Sea Resources*, Taylor & Francis Group, London, 825-834. https://doi.org/10.1201/b15813-103

[21] Mishra, A.K. and Kumar, G.S. (2015) Weathering of Oil Spill: Modeling and Analysis. *Aquatic Procedia*, **4**, 435-442. https://doi.org/10.1016/j.aqpro.2015.02.058

[22] Keramea, P., Kokkos, N., Gikas, G.D. and Sylaios, G. (2022) Operational Modeling of North Aegean Oil Spills Forced by Real-Time Met-Ocean Forecasts. *Journal of Marine Science and Engineering*, **10**, Article No. 411. https://doi.org/10.3390/jmse10030411

[23] Beegle-Krause, C.J. (2005) General NOAA Oil Modeling Environment (GNOME): A New Spill Trajectory Model. *International Oil Spill Conference IOSC* 2005, Miami, 15-19 May 2005, 3277-3283.

[24] Lee, M. and Jung, J.-Y. (2015) Pollution Risk Assessment of Oil Spill Accidents in Garorim Bay of Korea. *Marine Pollution Bulletin*, **100**, 297-303. https://doi.org/10.1016/j.marpolbul.2015.08.037

[25] Olita, A., Cucco, A., Simeone, S., Ribotti, A., Fazioli, L., Sorgente, B. and Sorgente, R. (2012) Oil Spill Hazard and Risk Assessment for the Shorelines of a Mediterranean Coastal Archipelago. *Ocean & Coastal Management*, **57**, 44-52. https://doi.org/10.1016/j.ocecoaman.2011.11.006

[26] Saçu, Ş., Şen, O. and Erdik, T. (2021) A Stochastic Assessment for Oil Contamination Probability: A Case Study of the Bosphorus. *Ocean Engineering*, **231**, Article ID: 109064. https://doi.org/10.1016/j.oceaneng.2021.109064

[27] Iouzzi, N., Ben Meftah, M., Haffane, M., Mouakkir, L., Chagdali, M. and Mossa, M. (2023) Modeling of the Fate and Behaviors of an Oil Spill in the Azemmour River Estuary in Morocco. *Water* (*Switzerland*), **15**, Article No. 1776. https://doi.org/10.3390/w15091776

[28] Ahmed, M.G. and Elhassan, B.M. (2012) Modeling of Oil Spill Trajectory and Fate in Sudanese Red Sea Coastal Water Masoud. *Journal of Science and Technology*, **13**, 45-53.

[29] Zelenke, B., O'Connor, C., Barker, C., Beegle-Krause, C.J. and Eclipse, L. (2012) General NOAA Operational Modeling Environment (GNOME) Technical Documentation.

[30] SCA Suez Canal. https://www.suezcanal.gov.eg/

[31] IMO List of IMO Conventions. https://www.imo.org/en/about/Conventions/Pages/ListOfConventions.aspx

[32] Vankayalapati, K., Dasari, H.P., Langodan, S., El Mohtar, S., Sanikommu, S., Asfahani, K., Desamsetti, S. and Hoteit, I. (2023) Multi-Mission Satellite Detection and Tracking of October 2019 Sabiti Oil Spill in the Red Sea. *Remote Sensing*, **15**, Article No. 38. https://doi.org/10.3390/rs15010038

[33] Huynh, B.Q., Kwong, L.H., Kiang, M.V., Chin, E.T., Mohareb, A.M., Jumaan, A.O.,

Basu, S., Geldsetzer, P., Karaki, F.M. and Rehkopf, D.H. (2021) Public Health Impacts of an Imminent Red Sea Oil Spill. *Nature Sustainability*, **4**, 1084-1091. https://doi.org/10.1038/s41893-021-00774-8

[34] Chabi, N., Houma Bachari, F., Bachari, N.E.I. and Bouda, A. (2023) Oil Spill Vulnerable Areas in Arzew Gulf: A Study Case. *SN Applied Sciences*, **5**, Article No. 158. https://doi.org/10.1007/s42452-023-05376-x

[35] FAO (2008) Fishery Country Profile: Republic of Sudan.

[36] Sofianos, S.S. and Johns, W.E. (2002) An Oceanic General Circulation Model (OGCM) Investigation of the Red Sea Circulation, 1. Exchange between the Red Sea and the Indian Ocean. *Journal of Geophysical Research*: *Oceans*, **107**, 17-1-17-11. https://doi.org/10.1029/2001JC001184

[37] Essa, S., Harahsheh, H., Shiobara, M. and Nishidai, T. (2005) Chapter 3. Operational Remote Sensing for the Detection and Monitoring of Oil Pollution in the Arabian Gulf: Case Studies from the United Arab Emirates. In: *Developments in Earth and Environmental Sciences*, Vol. 3, Elsevier, Amsterdam, 31-48. https://doi.org/10.1016/S1571-9197(05)80027-8

[38] Abera, W., *et al.* (2020) Scientific Misconduct and Partisan Research on the Stability of the Grand Ethiopian Renaissance Dam: A Critical Review of a Contribution to Environmental Remote Sensing in Egypt (Springer, 2020). In: Melesse, A.M., Abtew, W. and Moges, S.A., Eds., *Nile and Grand Ethiopian Renaissance Dam*, Springer Geography, Springer, Cham, 273-293. https://doi.org/10.1007/978-3-030-76437-1_15

[39] Gerges, M.A. (2002) Marine the Red Sea and Gulf of Aden Action Plan—Facing the Challenges of an Ocean Gateway. *Ocean & Coastal Management*, **45**, 885-903. https://doi.org/10.1016/S0964-5691(02)00112-6

[40] Osman, A. and Elbashier, M.M.A. (2019) Mangroves in Sudanese Red Sea (Major Threats and Future): A Brief Review. *Interciencia Journal*, **44**, 110-132.

[41] Persga, J. (2004) Dungonab Bay-Mukawwar Island Proposed Marine Protected Area Site-Specific Master Plan with Management Guidelines.

[42] SPC Sea Ports Corporation—Sudan. https://sudanports.gov.sd/web/en/

[43] Wenning, R.J., Robinson, H., Bock, M., Rempel-Hester, M.A. and Gardiner, W. (2018) Current Practices and Knowledge Supporting Oil Spill Risk Assessment in the Arctic. *Marine Environmental Research*, **141**, 289-304. https://doi.org/10.1016/j.marenvres.2018.09.006

[44] Balogun, A.L., Yekeen, S.T., Pradhan, B. and Wan Yusof, K.B. (2021) Oil Spill Trajectory Modelling and Environmental Vulnerability Mapping Using GNOME Model and GIS. *Environmental Pollution*, **268**, Article ID: 115812. https://doi.org/10.1016/j.envpol.2020.115812

[45] Hudson, C. and Cho, J. (2019) Final Report: WebGNOME Trajectories ADIOS Oil Database Project.

[46] Uttieri, M., Cianelli, D., Nardelli, B.B., Buonocore, B., Falco, P., Colella, S. and Zambianchi, E. (2011) Multiplatform Observation of the Surface Circulation in the Gulf of Naples (Southern Tyrrhenian Sea). *Ocean Dynamics*, **61**, 779-796. https://doi.org/10.1007/s10236-011-0401-z

[47] Kim, T.H., Yang, C.S., Oh, J.H. and Ouchi, K. (2014) Analysis of the Contribution of Wind Drift Factor to Oil Slick Movement under Strong Tidal Condition: *Hebei Spirit* Oil Spill Case. *PLOS ONE*, **9**, e87393. https://doi.org/10.1371/journal.pone.0087393

[48] Momoh, S.J.B. (2021) Oil Spill Fate and Trajectory Simulation for Sierra Leone's

Offshore Exploration Basin, Using the Savanah-1X Well as the Focal Point. *International Oil Spill Conference Proceedings*, **2021**, Article ID: 690419. https://doi.org/10.7901/2169-3358-2021.1.690419

[49] Prasad, S.J.S., Balakrishnan Nair, T.M.T., Francis, P.A. and Vijayalakshmi, T. (2014) Hindcasting and Validation of Mumbai Oil Spills Using GNOME. *International Research Journal of Environmental Sciences*, **3**, 18-27.

[50] Beegle-Krause, C.J. (1999) GNOME: NOAA's Next-Generation Spill Trajectory Model. *Oceans Conference Record*, **3**, 1262-1266.

[51] Cheng, Y., Li, X., Xu, Q., Garcia-Pineda, O., Andersen, O.B. and Pichel, W.G. (2011) SAR Observation and Model Tracking of an Oil Spill Event in Coastal Waters. *Marine Pollution Bulletin*, **62**, 350-363. https://doi.org/10.1016/j.marpolbul.2010.10.005

[52] Boehm, P.D., Page, D.S., Brown, J.S., Neff, J.M., Bragg, J.R. and Atlas, R.M. (2008) Distribution and Weathering of Crude Oil Residues on Shorelines 18 Years after the Exxon Valdez Spill. *Environmental Science & Technology*, **42**, 9210-9216. https://doi.org/10.1021/es8022623

[53] Wheeler, R.B. (1978) The Fate of Petroleum in the Marine Environment.

[54] Iskander, L., Khalil, C.A. and Boufadel, M.C. (2020) Fate of Crude Oil in the Environment and Remediation of Oil Spills. *STEM Fellowship Journal*, **6**, 69-75. https://doi.org/10.17975/sfj-2020-013

[55] Samuels, W.B., Amstutz, D.E., Bahadur, R. and Ziemniak, C. (2013) Development of a Global Oil Spill Modeling System. *Earth Sciences Research*, **2**, 52-61. https://doi.org/10.5539/esr.v2n2p52

[56] Nasr, P. and Smith, E. (2006) Simulation of Oil Spills near Environmentally Sensitive Areas in Egyptian Coastal Waters. *Water and Environment Journal*, **20**, 11-18. https://doi.org/10.1111/j.1747-6593.2005.00013.x

[57] Wessel, P. and Smith, W.H.F. (1996) A Global, Self-Consistent, Hierarchical, High-Resolution Shoreline Database. *Journal of Geophysical Research*: *Solid Earth*, **101**, 8741-8743. https://doi.org/10.1029/96JB00104

[58] Belkin, I.M. (2009) Rapid Warming of Large Marine Ecosystems. *Progress in Oceanography*, **81**, 207-213. https://doi.org/10.1016/j.pocean.2009.04.011

[59] Mezger, E.M., de Nooijer, L.J., Boer, W., Brummer, G.J.A. and Reichart, G.J. (2016) Salinity Controls on Na Incorporation in Red Sea Planktonic Foraminifera. *Paleoceanography*, **31**, 1562-1582. https://doi.org/10.1002/2016PA003052

[60] Morales-Nin, B., Cannizzaro, L., Massuti, E., Potoschi, A. and Andaloro, F. (2000) An Overview of the FADs Fishery in the Mediterranean Sea. *Pêche Thonière et Dispositifs de Concentration de Poissons,* Caribbean-Martinique, 15-19 Octobre 1999, 184-207.

[61] Mesonet Wind Rose. https://mesonet.agron.iastate.edu/sites/locate.php?network=SD__ASOS%0A

[62] Dhaka, A. and Chattopadhyay, P. (2021) A Review on Physical Remediation Techniques for Treatment of Marine Oil Spills. *Journal of Environmental Management*, **288**, Article ID: 112428. https://doi.org/10.1016/j.jenvman.2021.112428

[63] Ju, X., Li, Z., Dong, B., Meng, X. and Huang, S. (2022) Mathematical Physics Modelling and Prediction of Oil Spill Trajectory for a Catenary Anchor Leg Mooring (CALM) System. *Advances in Mathematical Physics*, **2022**, Article ID: 3909552. https://doi.org/10.1155/2022/3909552

[64] Abdallah, I.M. and Chantsev, V.Y. (2022) Simulating Oil Spill Movement and Beha-

vior: A Case Study from the Gulf of Suez, Egypt. Model. *Earth Systems and Environment*, **8**, 4553-4562. https://doi.org/10.1007/s40808-022-01449-9

[65] Omar, M.Y., *et al.* (2020) Oil Spill Modeling at Sidi Kreir SUMED Oil Terminal, Alexandria, Egypt. *Advanced Intelligent Systems for Sustainable Development* (*AI2SD*'2019), Volume 4, 331-341.

[66] PERSGA (2004) Sanganeb Marine National Park Site-Specific Master Plan with Management Guidelines.

[67] Lončar, G., Paklar, G.B. and Janeković, I. (2012) Numerical Modelling of Oil Spills in the Area of Kvarner and Rijeka Bay (The Northern Adriatic Sea). *Journal of Applied Mathematics*, **2012**, Article ID: 497936. https://doi.org/10.1155/2012/497936

[68] Scholz, D.K., Kucklick, J.J., Pond, R., Walker, A.H, Bostrom, A. and Fischbeck, P. (1999) Fate of Spilled Oil in Marine Waters: Where Does It Go? What Does It Do? How Do Dispersants Affect It? 1-57.

[69] Salm, R. V., Done, T. and McLeod, E. (2011) Marine Protected Area Planning in a Changing Climate. In: *Coral Reefs and Climate Change*: *Science and Management*, American Geophysical Union, Washington DC, 207-221.

[70] Omar, M.Y., Shehada, M.F., Mehanna, A.K., Elbatran, A.H. and Elmesiry, M.M. (2021) A Case Study of the Suez Gulf: Modelling of the Oil Spill Behavior in the Marine Environment. *The Egyptian Journal of Aquatic Research*, **47**, 345-356. https://doi.org/10.1016/j.ejar.2021.10.005

[71] Afenyo, M., Veitch, B. and Khan, F. (2016) A State-of-the-Art Review of Fate and Transport of Oil Spills in Open and Ice-Covered Water. *Ocean Engineering*, **119**, 233-248. https://doi.org/10.1016/j.oceaneng.2015.10.014

[72] Toz, A.C., Koseoglu, B. and Sakar, C. (2016) Numerical Modelling of Oil Spill in New York Bay. *Archives of Environmental Protection*, **42**, 22-31. https://doi.org/10.1515/aep-2016-0037

[73] Hook, S., Batley, G., Holloway, M., Ross, A. and Irving, P. (2016) Oil Spill Monitoring Handbook. CSIRO Publishing, Clayton. https://doi.org/10.1071/9781486306350

[74] Das, K. and Mukherjee, A.K. (2007) Crude Petroleum-Oil Biodegradation Efficiency of *Bacillus subtilis* and *Pseudomonas aeruginosa* Strains Isolated from a Petroleum-Oil Contaminated Soil from North-East India. *Bioresource Technology*, **98**, 1339-1345. https://doi.org/10.1016/j.biortech.2006.05.032

[75] Pradhan, B., Das, M. and Pradhan, C. (2021) Forecasting Oil Spill Movement through Trajectory Modeling: A Case Study from Bay of Bengal, India. Model. *Earth Systems and Environment*, **7**, 1107-1119. https://doi.org/10.1007/s40808-020-00933-4

[76] Hajivand, P. and Vaziri, A. (2015) Optimization of Demulsifier Formulation for Separation of Water from Crude Oil Emulsions. *Brazilian Journal of Chemical Engineering*, **32**, 107-118. https://doi.org/10.1590/0104-6632.20150321s00002755

[77] Dave, D. and Ghaly, A.E. (2011) Remediation Technologies for Marine Oil Spills: A Critical Review and Comparative Analysis. *American Journal of Environmental Sciences*, **7**, 424-440. https://doi.org/10.3844/ajessp.2011.424.440

[78] Boyd, J.N., Scholz, D. and Walker, A.H. (2005) Effects of Oil and Chemically Dispersed Oil in the Environment. *International Oil Spill Conference IOSC* 2005, Miami, 15-19 May 2005, 2329-2332.

[79] Toz, A.C. and Koseoglu, B. (2018) Trajectory Prediction of Oil Spill with Pisces 2 around Bay of Izmir, Turkey. *Marine Pollution Bulletin*, **126**, 215-227. https://doi.org/10.1016/j.marpolbul.2017.08.062

Appendices

Table 1. Rates of evaporation, dispersion, beached, and floating in hours for the first scenario, January, winter.

Time (hours)	Evaporated (%)	Dispersion (%)	Beached (%)	Floating (%)
1	47.7	0.0	0	51.9
2	49	0.2	0	50.4
3	49.5	0.4	0	49.7
4	49.9	0.6	0	49.2
5	50.3	0.7	0	48.8
6	50.6	0.8	0	48.4
9	51.5	0.9	0	47.4
12	52.2	1	0	46.7
15	52.8	1	0	46.1
18	53.2	1	0	45.7
21	53.6	1	0	45.3
24	53.9	1	0	45
30	54.5	1	0	44.4
36	54.9	1	8.4	35.6
42	55.3	1	7.6	36
48	55.7	1	8	35.2
60	56.5	1	7.8	34.6
72	57.2	1	7.5	34.2
84	58	1	7.5	33.4
96	58.7	1	7.5	32.8
108	59.3	1	7.5	32.1
120	60	1	7.5	31.4

Table 2. Rates of evaporation, dispersion, beached, and floating in hours for the second scenario, July, summer.

Time (hours)	Evaporated (%)	Dispersion (%)	Beached (%)	Floating (%)
1	45.3	0	0	54.7
2	49.1	0	0	50.9
3	50	0.1	0	49.9
4	51	0.2	0	48.8
5	51.9	0.3	0	47.8
6	52.7	0.6	0	46.8
9	54.5	0.6	0	44.9
12	56.1	0.6	0	43.3
15	57.5	0.7	0	41.8
18	58.7	0.7	0	40.7
21	59.8	0.7	0	39.5
24	60.7	0.7	0	38.5
30	61.9	0.8	0	37.2
36	62.6	0.8	0	36.5
42	63	0.8	0	36.1
48	63.2	0.8	0	35.9
60	63.5	0.8	0	35.6
72	63.8	0.8	0	35.3
84	64.1	0.8	0	35.1
96	64.3	0.8	0	34.9
108	64.4	0.8	0	34.7
120	64.6	0.8	0	34.5